JTTEE5 17:199–213
DOI: 10.1007/s11666-007-9148-y
1059-9630/$19.00 © ASM International

Technical and Economical Aspects of Current Thermal Barrier Coating Systems for Gas Turbine Engines by Thermal Spray and EBPVD: A Review

Albert Feuerstein, James Knapp, Thomas Taylor, Adil Ashary, Ann Bolcavage, and Neil Hitchman

(Submitted June 19, 2007; in revised form August 17, 2007)

The most advanced thermal barrier coating (TBC) systems for aircraft engine and power generation hot section components consist of electron beam physical vapor deposition (EBPVD) applied yttria-stabilized zirconia and platinum modified diffusion aluminide bond coating. Thermally sprayed ceramic and MCrAlY bond coatings, however, are still used extensively for combustors and power generation blades and vanes. This article highlights the key features of plasma spray and HVOF, diffusion aluminizing, and EBPVD coating processes. The coating characteristics of thermally sprayed MCrAlY bond coat as well as low density and dense vertically cracked (DVC) Zircoat TBC are described. Essential features of a typical EBPVD TBC coating system, consisting of a diffusion aluminide and a columnar TBC, are also presented. The major coating cost elements such as material, equipment and processing are explained for the different technologies, with a performance and cost comparison given for selected examples.

Keywords advantages of TS, APS coatings, coatings for gas turbine components, TBC topcoats, thermal properties review

1. Introduction

Thermal barrier coating systems (TBCs) are widely used in modern gas turbine engines to lower the metal surface temperature in combustor and turbine section hardware. Engines for both aero-jet propulsion and land-based industrial power generation have taken advantage of this technology to meet increasing demands for greater fuel efficiency, lower NO_x emissions, and higher power and thrust. The engine components exposed to the most extreme temperatures are the combustor and the initial rotor blades and nozzle guide vanes of the high-pressure turbine. Metal temperature reductions of up to 165 °C are possible when TBCs are used in conjunction with external film cooling and internal component air cooling (Ref 1). In film cooling a protective blanket of cooling air is ejected onto the external surface of the turbine vane or blade, from internal passages within the airfoils, by means of holes or slots in the surface. Figure 1 is a schematic of the key elements of an aircraft gas turbine, with the pressure and temperature profiles present along the gas path from air intake to exhaust. A diagram of the relative temperature reduction achieved using both TBC and cooling air technologies on hot section hardware is shown in Fig. 2.

A typical TBC consists of two key layers: an oxidation resistant bond coat such as diffusion aluminide or overlay MCrAlY bond coating, and a ceramic top layer, typically 7-8 wt.% Y_2O_3-stabilized ZrO_2 (7YSZ), to reduce the heat flux into the component.

The ceramic top layer is typically applied either by plasma spray or by electron beam physical vapor deposition (EBPVD) (Ref 2, 3). Significant effort is going into the development of new ceramic compositions with lower thermal conductivity. Concepts used are advanced multi-component zirconia (ZrO_2)-based TBCs using an oxide defect clustering design and materials whose compositions have a pyrochlore structure (Ref 4, 5). In addition to a low-thermal conductivity, other desired properties of a thermal barrier coating are also phase stability during long term high-temperature exposure and thermal cycling, resistance to erosion and pollutants such as, e.g., CMAS, which can destroy the integrity of the thermal barrier coating by infiltrating the pores and react with the coating.

An aluminum-enriched bond coat composition is used to provide a slow growing, adherent aluminum oxide film, otherwise known as a thermally grown oxide, or TGO (Ref 6). This alumina scale is an ideal oxygen diffusion barrier, since it has one of the lowest oxygen diffusion rates of all protective oxide films (Ref 7).

Bond coat oxidation is the primary cause of TBC failure (Ref 8). Thermal cycling testing has shown the modes of failure to include the growth of a delamination crack in the zirconia layer just above the TGO and bond coat,

Albert Feuerstein, James Knapp, Thomas Taylor, Adil Ashary, and **Neil Hitchman**, Praxair Surface Technologies, Inc., Indianapolis, IN USA; and **Ann Bolcavage**, Rolls Royce Corporation, Indianapolis, IN USA. Contact e-mail: albert_feurstein@praxair.com.

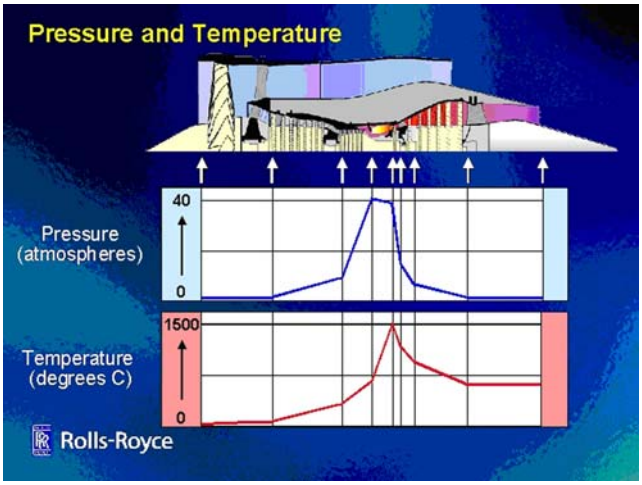

Fig. 1 A gas turbine engine schematic, showing the different sections along the engine along with corresponding pressure and temperature profiles. Diagram after Michael Cervenka, Rolls-Royce Corporation, 2001

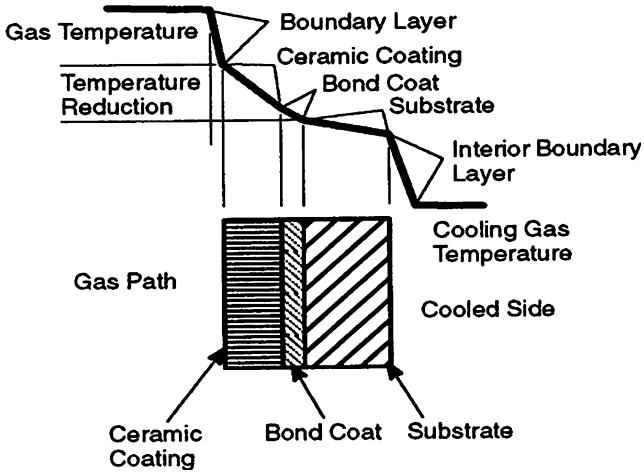

Fig. 2 Schematic of a TBC on an air-cooled gas turbine engine component (Ref 2). The thermal barrier acts as a heat flow resistor and is only efficient in cooled engine components

cracking within the TGO, and at the TGO/bond coat interface (Ref 9-11).

This article concentrates on TBCs for selected high-temperature applications in a modern gas turbine engine. Specifically, the key features of each layer which affect performance, common deposition technologies, and the economic factors that must be considered, are addressed.

2. Modern Ceramic Thermal Barrier Coatings

Presently essentially two types of application methods are used to deposit the 7YSZ ceramic layer onto commercial gas turbine engine components. Plasma spray deposition is commonly utilized to deposit TBCs onto components such as combustor hardware, turbine outer air seal ring segments, and stationary nozzle guide vanes. Rotating blades and some high-pressure turbine section vanes, which require surfaces with a smooth finish and the ability to withstand a high degree of thermo-mechanical strain, are often coated using EBPVD technology. Alternate thermal spray technologies using liquid precursors show promising results and potential, but need still optimization work (Ref 12).

2.1 Plasma-Sprayed Ceramic Thermal Barrier Coatings

A ceramic top layer deposited by air plasma spray (APS) consists of either of two morphologies. A ''low density'' coating exhibits an even spacing of pores and voids ranging from 20 μm to nanosized, with sub-critical horizontal micro-cracking between individual splat layers. These features, along with the inherent phonon scattering properties of the 7YSZ atomic lattice, aid in reducing heat flux transfer to the metallic bond coat and component. The coating density usually ranges between 80 and 86% of the theoretical value. Figure 3 shows optical and SEM images of a typical low-density coating in cross section.

Alternatively, dense, vertically segmented coatings, such as Zircoat (Praxair Surface Technologies, Inc.) (Ref 13) shown in Fig. 4, are successfully used in both aircraft and land-based gas turbine engines (Ref 14). Dense, vertically macro-cracked TBCs provide improved tolerance of the ceramic layer to the strain caused by the CTE mismatch of ceramic and bond coat. The vertical segments are in the primary direction of the conductive heat flow, and thus do not inhibit conductive heat transfer through the coating thickness.

As in the case of APS low density coatings, horizontal splat boundaries and porosity, as well as a limited amount of horizontal crack branching from the vertical segments of Zircoat, influence the defect-generated contribution to the thermal conductivity.

2.2 EBPVD Ceramic Thermal Barrier Coatings

EBPVD TBCs, consisting of a fine columnar microstructure, are utilized in the most advanced gas turbine engines. The loosely bonded columnar grains, presented in Fig. 5, serve the same purpose as vertical crack segments in plasma-sprayed coatings, and provide a high degree of mechanical compliance. However, the lack of large splat boundaries and other features normal to the heat flow direction ensures that 7YSZ EBPVD TBCs will have relatively higher thermal conductivity values vs. their plasma-sprayed counterparts of the same composition (Ref 9).

The 7YSZ EBPVD TBC polished cross section in Fig. 5 shows a plurality of fine columnar grains nucleating on top of the aluminide bond coat. These subsequently increase in size during the vapor deposition process due to competitive growth. The fracture surface in Fig. 6 contains a fine profusion of micro-columns which collectively constitute each columnar grain. Even at this level of magnification, there are no discernable horizontally oriented

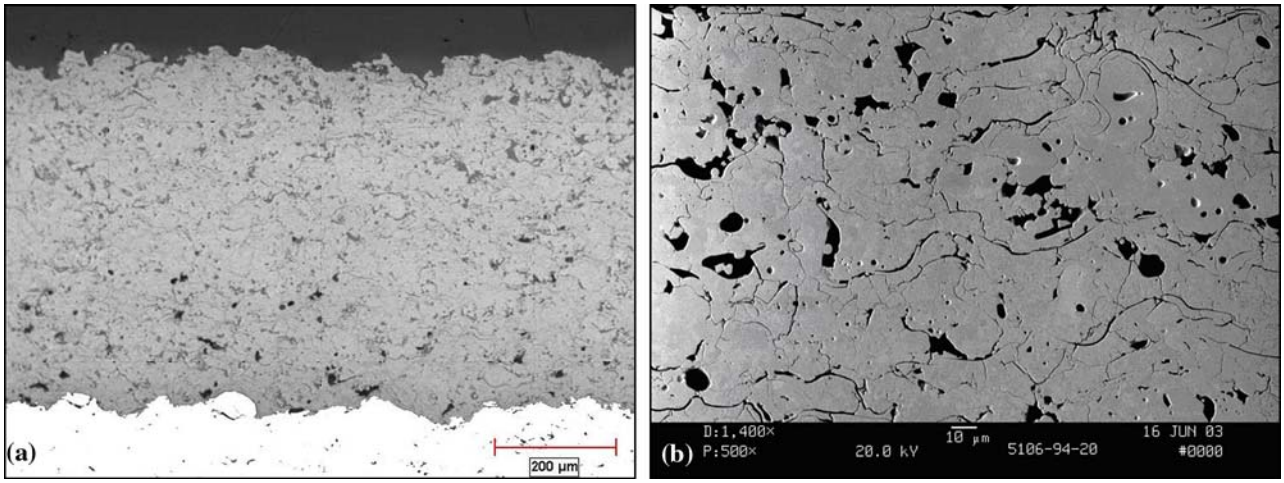

Fig. 3 (a) and (b): Cross section of APS low density TBC, containing approximately 15% porosity. Two different magnifications are shown to reveal the ''macro'' and ''micro'' structure of the coating

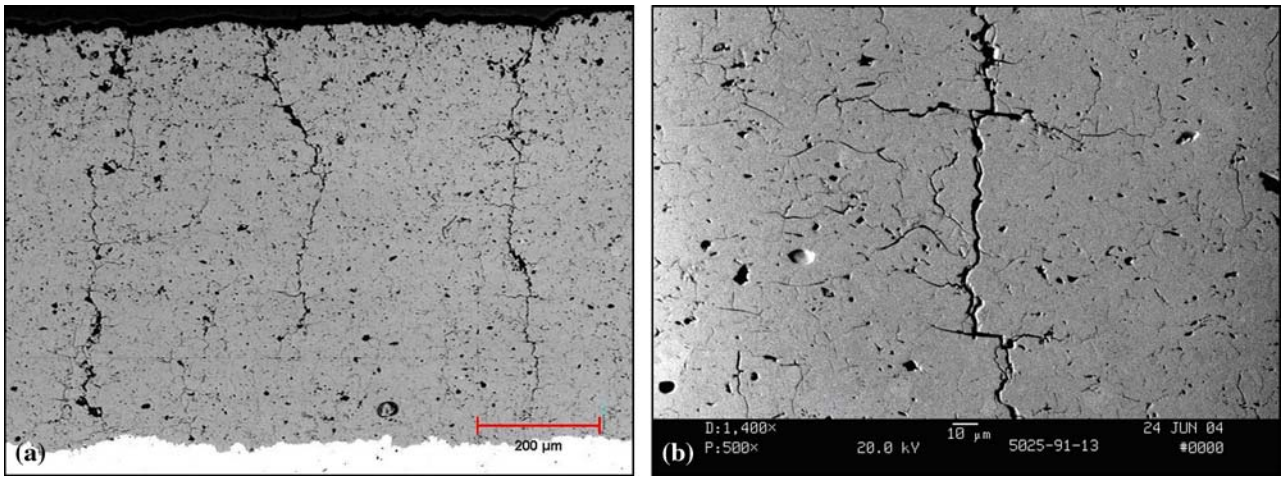

Fig. 4 (a) and (b): Cross section of APS Zircoat TBC, containing approximately 16-24 cracks per linear centimeter. Two different magnifications are shown to reveal the ''macro'' and ''micro'' structure of the coating

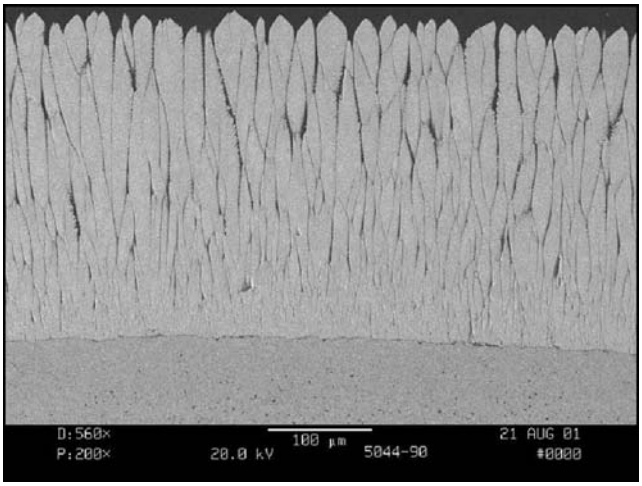

Fig. 5 EBPVD TBC, featuring a plurality of vertical, loosely bonded columnar grains

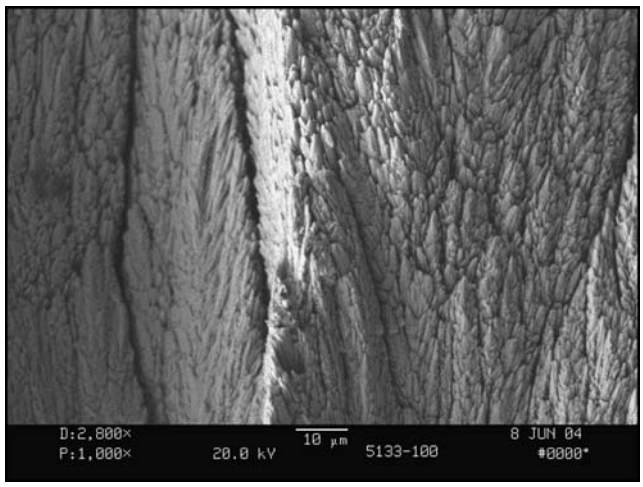

Fig. 6 SEM image of a 7YSZ EBPVD TBC fracture surface

Table 1 Average thickness, density, and room temperature thermophysical data of 7YSZ coatings

TBC description	Thickness, µm	Density g/cm^3	Density % Bulk	Diffusivity at 23 °C, cm^2/s	Conductivity at 23 °C, W/m K
YSZ—low density	262	5.14	85.0	0.00338	0.83
YSZ—Zircoat	724	5.56	91.8	0.00547	1.46
YSZ—EBPVD	144	4.68	77.7	0.0768	1.71

All measurements were taken at normal air pressure. The value for the specific heat was measured at 0.489 Ws/g K

features that would impede conductive heat flow through the coating.

2.3 Thermal Conductivity of APS and EBPVD TBC

TBC coatings deposited by APS offer a thermal conductivity significantly lower (0.9-1.1 W/m K), than that of fully dense, monolithic 7YSZ (>2 W/m K), as the boundaries and pores tend to lie parallel to the surface and therefore perpendicular to the temperature gradient. By contrast, although the thermal conductivity of EBPVD TBC is not as low (1.7-1.8 W/m K) as that of APS coatings, EBPVD TBCs are nevertheless preferred for thin aero blade TBCs because of the strain tolerance imparted by the microstructure.

Thermal conductivity is primarily affected by the density of the coating, the number of internal boundaries and pores. The orientation of the internal cracks and pores relatively to the thermal flux is also critical. In order to calculate thermal conductivity, one must also know the specific heat of that particular ceramic composition, the density, and the thermal diffusivity as a function of temperature (measured using the laser flash technique, Ref 15). More specific details on these techniques are published elsewhere (Ref 16, 17).

A list of the thickness and density of typical TBC morphologies, as well as the resulting room temperature thermal diffusivity and thermal conductivity data measured with the laser flash method, is shown in Table 1. Density measurements are expressed as both measured values in g/cm^3 and as a percentage of the bulk value.

Specific heat was measured using a standard Perkin-Elmer Model DSC-2 Differential Scanning Calorimeter with sapphire as the reference material (ASTM E1269). The standard and sample were subjected to the same heat flux as a blank and the differential powers required to heat the sample and standard at the same rate were determined using the digital data acquisition system. From the masses of the sapphire standard and sample, the differential power, and the known specific heat of sapphire, the specific heat of the sample is computed.

The thermal conductivity values measured at normal atmospheric air pressure and at each temperature on heating are shown in Fig. 7. Data points obtained upon cooling in these coatings showed no significant rise in thermal conductivity due to sintering effects, due to the short amount of time at high temperature.

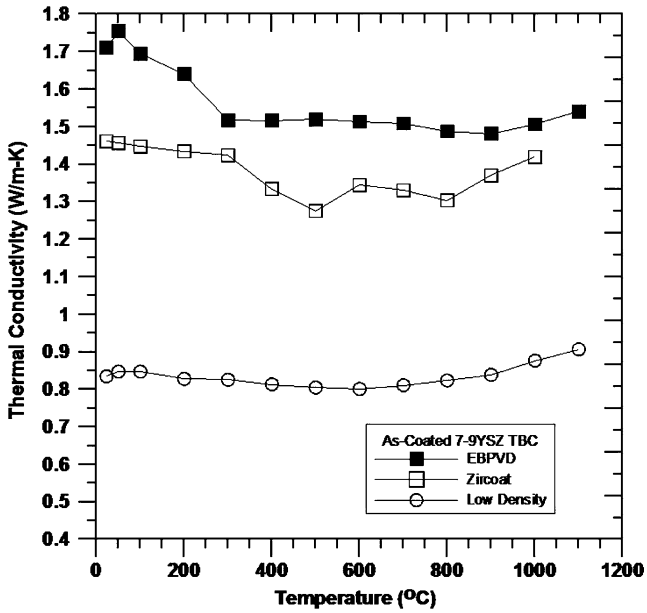

Fig. 7 Temperature dependence of thermal conductivity for 7YSZ TBCs

It is worthwhile to mention that the thermal conductivity of a porous material may be affected by the external gas pressure, according to the pore size and morphology. Thus the thermal conductivity of APS coatings typically increases with increasing pressure, as it is the case in the engine, whereas EB-PBD thermal conductivity is almost pressure independent. This aspect is of prime importance as the measurement conditions (temperature and pressure) of the thermal conductivity are in general far from those in service (as it is well shown on Fig. 1).

It is also important to mention that the thermal conductivity increases with long time thermal aging of the coatings (APS as well as EB-PVD coatings) due to (i) sintering effects, (ii) phase transformations in 7YSZ. Actually, this is a main issue which justifies the today search for new ceramic coatings with low conductivity AND increased stability (Ref 18, 19).

3. Bond Coat

The term bond coat may imply that diffusion aluminide or MCrAlY coatings are applied only for increased adherence of the TBC coating to the substrate alloy. Although these coatings do enhance the bonding between alloy and TBC, their primary function is to increase the high-temperature oxidation and corrosion resistance of underlying structural alloy.

High-temperature alloys derive their protection against oxidizing environments by forming a thin oxide layer commonly termed as a TGO. This layer acts as a barrier between the alloy and the atmosphere, and impedes further oxidation. Growth of the TGO occurs either by outward diffusion of metal ions or by inward diffusion of oxygen ion through the oxide layer.

The oxides which allow minimal diffusion grow slowly and thus provide maximum protection to the underlying alloy. The most commonly used TGOs for protection of high-temperature commercial alloys are α-alumina (Al_2O_3) and chromia (Cr_2O_3). These oxides have slow growth rates and due to their higher thermodynamic stability, are easily formed on metallic alloys. Chromia has higher growth rates than alumina, but has the disadvantage of forming gaseous CrO_3 at temperatures above 1000 °C. Presently, most advanced alloys and metallic coating rely on forming alumina scale for high-temperature protection. Also, a significant amount of chromium can be added to the alloys and coatings for high-temperature corrosion resistance.

Additions of large amounts of aluminum in structural alloys (greater than about 6 wt.%) to form protective alumina scale can adversely affect the mechanical properties. Furthermore, additions of refractory elements such as tantalum, tungsten, and rhenium in advanced alloys systems are made at the expense of chromium and aluminum. Diffusion aluminide and thermal spray overlay coatings, on the other hand, can contain large amount of aluminum, because they do not have to provide structural strength to the engine components. Diffusion aluminide coatings can contain up to 30 wt.% aluminum, and most thermally sprayed MCrAlY coatings contain 10 to 12 wt.% aluminum.

3.1 Diffusion Aluminide

Diffusion aluminide coatings are based on the intermetallic compound β-NiAl. Pack cementation is a commonly used process, because it is relatively inexpensive and capable of coating many small parts in one batch.

The parts are immersed in a powder mixture, containing alumina and aluminum particles, and ammonium halide activator. Coating takes place at temperatures between 800 and 1000 °C. Aluminum halides react on the surface of the part and deposit aluminum.

More advanced processes consist of ''over the pack'' vapor phase aluminizing (VPA) or chemical vapor deposition (CVD). These processes can control the flow of the aluminum halides to selected areas of the parts to be coated, and are used especially when there is a need to coat also the internals of components.

Depending on the activity of the aluminum and the coating temperature, one can achieve two coating microstructures (Ref 20). The low activity—high-temperature process (1050-1100 °C), forms NiAl by outward diffusion of nickel.

In the high activity—low temperature process (700-950 °C), Ni_2Al_3 and possibly β-NiAl forms by inward diffusion of aluminum. Typically a diffusion heat treatment is applied to form a fully homogeneous β-NiAl layer.

3.2 Platinum Aluminide

The addition of platinum to the diffusion aluminide coating system is beneficial in two ways: First, the platinum enhances the diffusion of aluminum (Ref 21) into the substrate alloy during the diffusion aluminizing process. Second, it significantly improves the oxidation properties of the aluminide coating (Ref 22). Typically 5 to 10 μm Pt is deposited by electroplating, followed by a diffusion aluminide process.

Platinum aluminide can also be made either with the low activity—high-temperature process or by the high activity—low-temperature diffusion process. Figures 8 and 9 show schematically the microstructures of these two types of coatings. Since the part surface is grit blasted prior to the application of the platinum, grit inclusions can serve as markers to indicate the additive coating layer or the original alloy surface. In the case of the low activity—high-temperature process, the additive layer is above the nickel diffusion zone, and in the case of high activity—low-temperature process, the additive layer is under the original surface marked by the grit inclusions. The relative thickness of the nickel diffusion zone also indicates the degree of outward diffusion of nickel. As the coating grows inwardly in the high activity—low-temperature process, it traps the carbides and other inclusions near the original alloys surface, as shown in Fig. 9. These inclusions can have a deleterious effect in that they can lower the oxidation/corrosion resistance of the coating.

In either processes, platinum aluminide can be single phase ((Ni, Pt)-Al) or double phase ((Ni, Pt)-Al + $PtAl_2$). The $PtAl_2$ secondary phase is schematically shown in

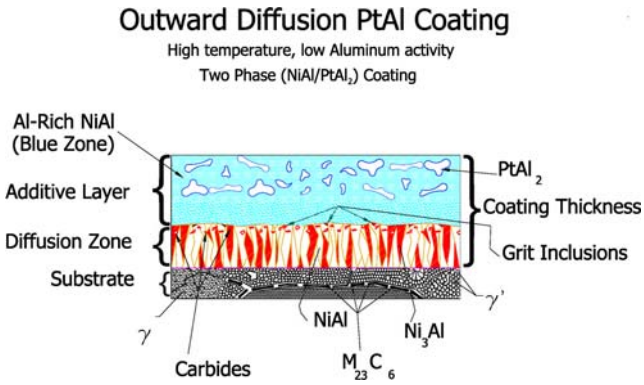

Fig. 8 Microstructure schematic showing platinum aluminide formed from a low activity—high-temperature process

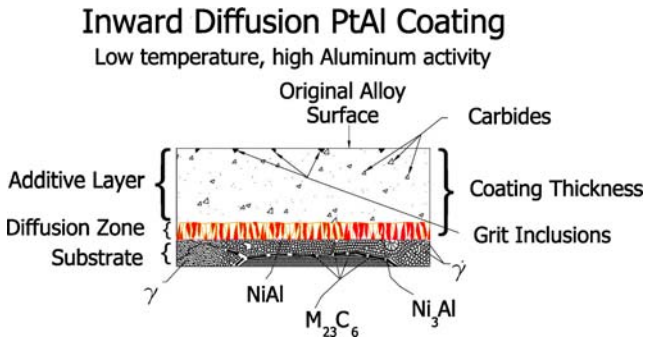

Fig. 9 Microstructure schematic showing platinum aluminide formed from a high activity—low-temperature process

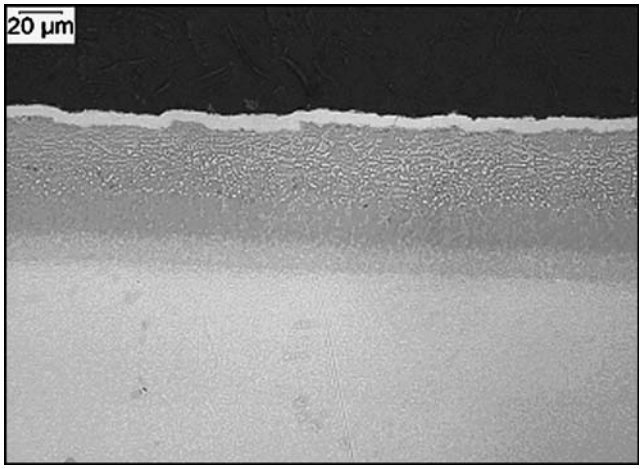

Fig. 10 Optical micrograph of an outwardly grown platinum aluminide diffusion coating. The top thin white layer is electroplated nickel, used for edge retention during metallographic preparation of the sample

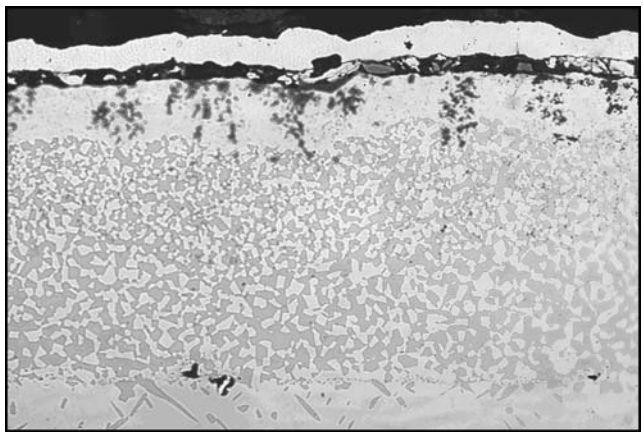

Fig. 11 Micrograph of a typical two-phase NiCoCrAlY bond coating, applied using LPPS, after several hours in service. The aluminide phase (*dark*) is depleted near the coating surface, and oxide pegs protrude from the TGO into the bond coating

Fig. 8. Figure 10 is a cross section SEM micrograph of a two-phase platinum aluminide coating. Although existence of the $PtAl_2$ phase ensures sufficient platinum in the coating, excess $PtAl_2$ can be detrimental, as it makes the coating brittle. A ''blue zone'' (as it appears in the optical microscope) is characteristic for the outer region of the additive layer. It also indicates the coating to be on the aluminum rich side of β-NiAl phase.

Important characteristics of platinum aluminide coatings are overall thickness, platinum and aluminum concentrations, thickness of the diffusion zone, and the amount of $PtAl_2$ phase. Coating thickness, which typically includes the diffusion zone, ranges from 50 to 100 µm.

Since aluminide coatings strongly interact with the underlying substrate via diffusion, the formation of brittle phases and the formation of a fast growing secondary reaction zone (SRZ) must be avoided. Therefore, each aluminide deposition process must be specifically tailored for different superalloy compositions.

3.3 MCrAlY Overlay Bond Coatings

The first commercial MCrAlY alloy was an iron-based FeCrAlY formulated by Pratt and Whitney in the late 1960s (Ref 23). Soon thereafter, they also patented CoCrAlY (Ref 24) and NiCoCrAlY compositions (Ref 25). Initially, MCrAlY coatings were applied either by vacuum induction or EBPVD. Primarily used as airfoil coatings, they were very successful in enhancing the oxidation and hot-corrosion resistance of gas turbine hardware. However, due to cost considerations, coatings manufacturers soon developed techniques such as air, vacuum, and low-pressure plasma spraying (APS, VPS, and LPPS) and high-velocity oxy-fuel (HVOF) deposition. Union Carbide (now PST) developed an inert gas shrouded plasma spray process for MCrAlY and other oxygen-reactive coatings (Ref 26) which maintained oxygen pickup to below 0.1 wt.%. Most recently, MCrAlY coatings have also been produced by Tribomet (Praxair Surface Technologies, Inc.) (Ref 27), a Ni or Co electroplating process with CrAlY powder entrapment and subsequent diffusion heat treatment. Uses for the coatings also expanded to other high-temperature applications in gas turbine and internal combustion engines, such as turbine shrouds (abradable and rub tolerant coatings), abrasive blade tips, and thermal barrier coating (TBC) bond coatings.

Overlay coatings compared to diffusion coatings provide more independence from the substrate alloy and more flexibility. The coating composition can be adjusted according to the expected degradation mechanisms in service. MCrAlY bond coatings contain typically four or more elements. Chromium gives these coatings excellent corrosion resistance combined with good oxidation resistance. After the coating deposition, a vacuum heat treatment provided a diffusion bonding for optimum adhesion.

MCrAlY coatings generally show a two-phase microstructure $\beta + \gamma$ (NiAl + Ni). The presence of continuous matrix fcc γ-phase increases its ductility and thus the thermal fatigue strength. The β-phase is the main reservoir of the aluminum in the coating. With increasing TGO thickness the aluminum rich phase in the outer region of the coating depletes and the γ-phase predominates (Ref 28). Figure 11 shows a cross section of a coating after an extended period of oxidation. The β-depleted region also shows a vast array of oxide protrusions.

These oxide protrusions sometimes form from the oxidation of reactive elements such as yttrium or hafnium. The reactive element oxide protrusions are called ''pegs,'' and are thought to be one of several mechanisms responsible for the enhanced adhesion of the alumina scales. MCrAlY alloys are effective because they are thermally and chemically compatible with their substrates and have a minimal effect on base-metal properties. Performance is attributed to their ability to form a tenacious, protective scale that inhibits any interactions between the host surface and the outside corrosive environment. The primary protective scale is aluminum oxide. Although

other elements in the coating can also form oxides, they are not as protective as alumina. Accordingly, their formation is discouraged by proper alloying of the MCrAlY.

Scale formation is related to the aluminum's activity and its diffusivity in the alloy. This activity is increased by chromium. Chromium (17-25 wt.%) also lowers the amount of aluminum needed to form and maintain the protective oxide film and also provides excellent corrosion resistance. A schematic diagram showing the relative oxidation and corrosion resistance of the most common overlay MCrAlY and diffusion aluminide coatings is shown in Fig. 12.

The aluminum in MCrAlY, usually between 8 and 12 wt.%, forms the oxide scale. In general, it is desirable to provide a slow growing well adherent pure alumina scale (TGO). As a major constituent of the alloy, it provides a reservoir from which the alumina scale is repeatedly replenished.

Elements beneficial for the scale adherence are reactive elements such as yttrium, hafnium, and zirconium. Thus, all MCrAlY coatings usually contain 1 wt.% yttrium or less. The mechanism of yttrium enhancement of MCrAlY oxidation resistance is still debated. Several studies have attributed yttrium's beneficial effects to modification of the alumina mechanical properties, pegging of the alumina to the metallic layer, or gettering of sulfur impurities which migrate from the bond coat or superalloy substrate (Ref 30, 31). Additions of hafnium and zirconium play a similar role, they also seem to prevent spallation of the TGO (Ref 32).

Work at the University of Pittsburgh has shown that the alumina scale on FeCrAlY coatings is fine grained and columnar, but not textured. In contrast, α-alumina on FeCrAl is coarser grained and equiaxed, but also not textured. This difference was attributed to yttrium suppressing aluminum transport in the scale (Ref 33). It is possible to add too much yttrium, and additions at and above 1 wt.%, the oxide scale is not alumina but yttrium aluminum garnet, which is not as protective as alumina.

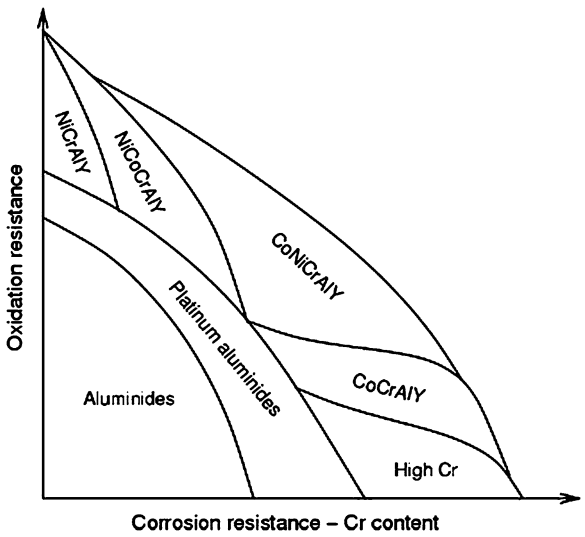

Fig. 12 Common MCrAlY and diffusion aluminide coating compositions in relation to oxidation and hot-corrosion resistance, after M. Schütze (Ref 29)

The effect of other additions beyond those found within the most common MCrAlY alloys has also been investigated. Additions of rhenium (Re) have been shown to improve isothermal or cyclic oxidation resistance, and thermal cycle fatigue (Ref 34). The amount of silicon (Si) added to any MCrAlY alloy must be limited. Too much will substantially lower the alloy's melting range. However, in small amounts, it has been shown to promote alumina scale adherence and, in some cases, form an oxide film of its own. The refractory metal tantalum is sometimes added to a MCrAlY coating to improve the alloy's high-temperature capabilities and resistance to sulfidation and hot corrosion. Platinum, though very expensive, is often added to a MCrAlY coating to increase its oxidation and hot-corrosion properties for operating at temperatures up to 2000°F (1093 °C). With regard to trace elements, considerable attention is now paid to minimizing sulfur, in some cases to well below 10 ppm (Ref 35). Sulfur has shown to be detrimental for the adherence of the thermally grown alumina scale.

4. Coating Process Technologies

In the following, we concentrate on selected TBC systems as applied at Praxair Surface Technologies for aero and industrial power gas turbines, and their related deposition processes. Table 2 lists the presently used combinations for these three key applications.

4.1 Plasma-Spray Coating of Combustors, Blades, and Vanes

A plasma-spray booth for applying TBCs onto aerospace and IGT combustors consists not only of the physical enclosure and the equipment contained therein, such as torches, gas and power service lines, tooling, multi-axis robots for gun and/or part manipulation, and ventilation systems, but also external process control components such as control panels for power, gas flow regulation, and powder feeder settings. Other necessary capital equipment includes grit blasting and cleaning/inspection facilities for component pre-coating preparation, and may also incorporate heat treatment furnaces and stripping tanks. Both MCrAlY and YSZ ceramic layers are typically applied in the same booth in sequential order, although separately dedicated systems may be used.

Table 2 Selected examples of TBC systems for various gas turbine applications

Example	Bond coat	Topcoat
Aerospace combustor	NiCoCrAlY via shrouded plasma spray	Zircoat via air plasma spray
IGT HPT blade	NiCoCrAlY HVOF	Low-density YSZ via air plasma spray
Aerospace HPT blade	Platinum-aluminide via diffusion	Columnar YSZ via EBPVD

Fig. 13 Plasma TBC coating of an annular combustor

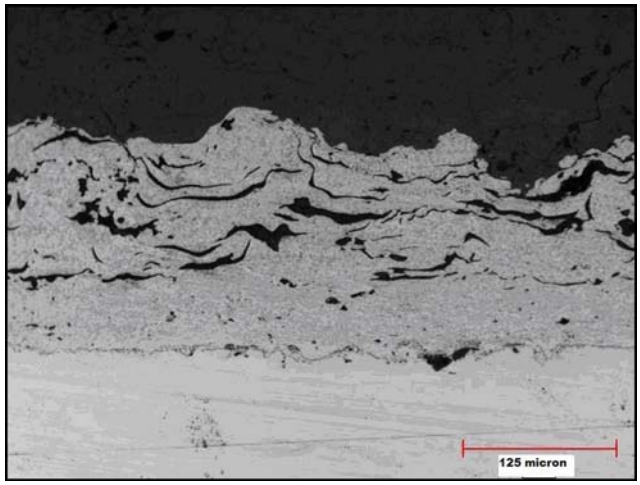

Fig. 14 Dual layer NiCrAlY bond coat (heat treated), with an average thickness of 150 μm, applied by the shrouded plasma process

For the coating of most annular combustors, a simple two-axis manipulator is sufficient to move the plasma torch and rotate the component. An example of a typical setup of this type is shown in Fig. 13, where a plasma torch attached to an extension arm is used to apply the ceramic YSZ layer on the inner diameter of a can-style combustor. Combustors with more complex geometry or with features far off-angle to the torch centerline require the use of robots and turntables or other manipulation equipment with multiple axes of movement.

The cost of applying coatings onto combustors via plasma spray is primarily influenced by two factors. First, the direct materials costs of MCrAlY powder, YSZ powder, and process gases are determined by the required thickness of each layer, the surface area to be coated, and the deposition efficiency of the plasma-spray process. Second, the cost of labor includes not only the operator's preparation of the coating booth and actual thermal spray time, but also preparation of components beforehand for thermal spray, such as inspection, cleaning, and grit blasting.

4.1.1 Bond Coating Deposition. Two bond coat deposition techniques are reviewed here, the Shrouded Plasma system and HVOF. Both systems have similarities in their requirements to provide an acceptable coating.

In order to provide optimum adherence for a TBC topcoat, a surface roughness of the MCrAlY bond coat at least approximately 10 μm Ra is desirable so as to mechanically anchor the layers together. This is usually accomplished by using a coarse powder with a size distribution within the range of 40 to 125 μm. A coating produced by a coarser powder, however, tends to exhibit porosity. If the bond coat has more than 6% porosity, even after vacuum heat treatment, any pores still inter-connected can result in accelerated internal oxidation of the coating once in service.

As the effluent emerges from the plasma torch, it is surrounded by an argon shroud to minimize the pickup of oxygen during flight to the component. With this proprietary design, oxygen content in argon-shrouded plasma spray deposited MCrAlY has been shown to contain an order of magnitude lower oxygen content in comparison to conventional air plasma-sprayed or HVOF-deposited MCrAlY coatings.

Accordingly, PST has historically applied a two-layer bond coat system (Ref 36) onto combustors and other aerospace and IGT components via gas-shrouded plasma spray (Ref 26), in conjunction with vacuum heat treatment. The inner layer is sprayed from a finer cut of powder, and sinters to at least 95% theoretical density during heat treatment. This layer has an average roughness of 5 μm, whereas a higher roughness for YSZ mechanical attachment is preferred. Therefore, the second layer of bond coat is added on top of the first, consisting of the same composition but of coarser powder, so as to produce a final roughness of at least 10 μm on the surface. Figure 14 shows a typical two-layer MCrAlY bond coat produced with shrouded plasma spray.

The HVOF deposition system comprises an oxygen and fuel mixture consisting of kerosene, propylene, propane, natural gas, or hydrogen, depending on the gun. The mixture of oxygen and fuel is injected into the combustion chamber and is ignited internally or externally from the gun. The powder is injected internally into the upper stream of the combustion flame, either axially or radially. The ignited gases form a circular flame, which surrounds the required coating powder as it flows through the nozzle. The combustion temperatures can exceed 2800 °C depending on gun operating parameters and the fuel type. The flame configuration shapes the powder stream to provide uniform heating and acceleration of the powder particles. Similar to the plasma spray process, the selection of gun parameters is based on providing the optimum heating and acceleration of the powder particles by the flame. Typical gas velocities are 1000 to 1200 m/s and can exceed 1500 m/s, depending on which hardware and spray parameters are utilized. To achieve the required bond coat

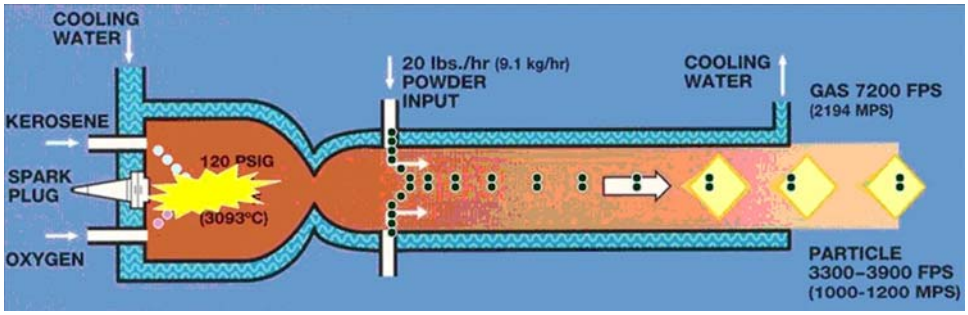

Fig. 15 Working principle of the Praxair TAFA JP5000 HVOF gun

density and surface roughness, MCrAlY applied with this technology can be either a single or dual layer. The schematic in Fig. 15 demonstrates the working principle of the Praxair TAFA JP5000 HVOF gun.

4.1.2 Thermal Barrier Coating Deposition. The ceramic TBC is applied onto the MCrAlY bond coating using plasma spray technology, with the resulting coating and its properties significantly influenced by the torch settings. YSZ ceramic powder is injected into the plasma effluent, heated, and accelerated toward the combustor surface. Where this injection takes place, in conjunction with other processing factors, dictates the TBC microstructure. Low-density TBCs, containing 15-20% pores, consist of multiple splat layers, along with a profusion of pores, voids, and sub-critical horizontal cracks between the splats. This microstructure is best obtained from plasma torches with powder injection ports externally positioned to the exit nozzle. Higher density, vertically segmented TBCs require a more complete treatment of the injected powder. This may be done through external injection with increased torch power, or through internal injection within the torch body.

4.2 TBC Systems for Combustors

Figure 16 shows an example of a TBC coating system for a combustor, consisting of a NiCrAlY bond coating and Zircoat ceramic top layer. Generally, MCrAlY bond coatings, whether single layer or dual-layer, are applied to thicknesses ranging from 125 to 250 μm. The thickness and type of thermal barrier layer is often dependent on the desired morphology, as well as the expected conditions in service. Low-density YSZ coatings typically range from 250 to 500 μm, although thicknesses up to 1000 μm are not uncommon in IGT combustors. Dense vertically segmented coatings are generally thicker, due to their higher thermal conductivity. Thicknesses above 500 μm are often recommended for good thermal insulation.

4.3 TBC Systems for IGT Components

The total coating thickness for IGT components ranges between 400 and 500 μm. Typically, HVOF is used at PST to apply the bond coating due to the large part size and long stand-off distances required during coating. A low-density TBC topcoat provides maximum thermal protection and good thermal shock resistance over extended time at high-operation temperatures. Plasma-sprayed ceramic thermal barriers are almost always employed. Figure 17 shows a TBC system for a typical IGT component, consisting of an HVOF-applied MCrAlY bond coat and an air-sprayed YSZ low-density topcoat, whereas Fig. 18 shows a large industrial vane receiving a HVOF bond coating.

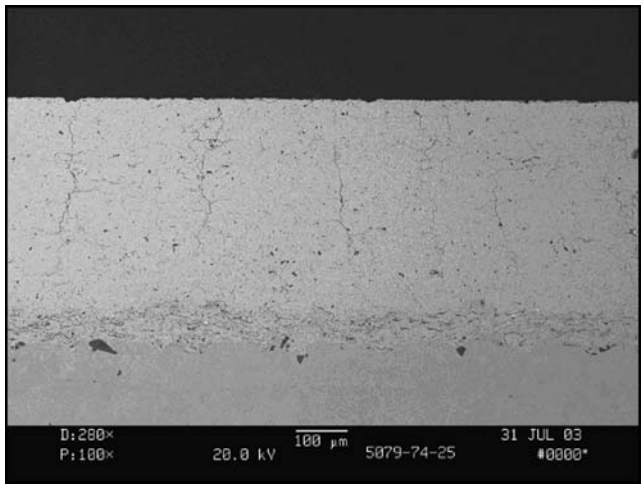

Fig. 16 Combustor TBC system consisting of Zircoat TBC and NiCrAlY bond coat. TBC surface was surface finished before metallographic evaluation

4.4 Platinum Aluminide/EBPVD TBC Systems

The platinum aluminide/EBPVD TBC system can be applied to a variety of modern aircraft and IGT parts, as shown in Fig. 19. The only limitation is whether the engine hardware can fit into and be easily handled within the various processing chambers. This TBC system requires three separate coating processes: electroplating, aluminizing, and EBPVD.

4.4.1 Platinum Aluminide Deposition. Platinum plating and diffusion aluminide are basically batch processes. Depending on the part size, 10 to 100 parts are processed simultaneously.

Parts are cleaned in a vapor degreaser; grit blasted, and weighed prior to platinum electroplating. The thickness of the platinum layer is controlled in terms of weight gain

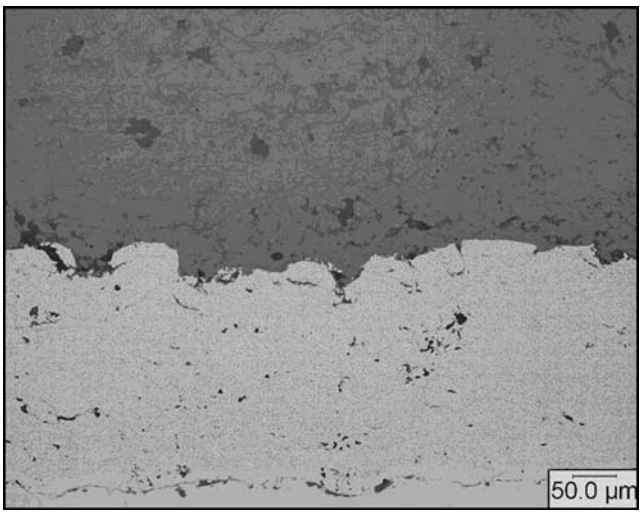

Fig. 17 IGT TBC coating system consisting of 2 layer HVOF bond coat and low density TBC

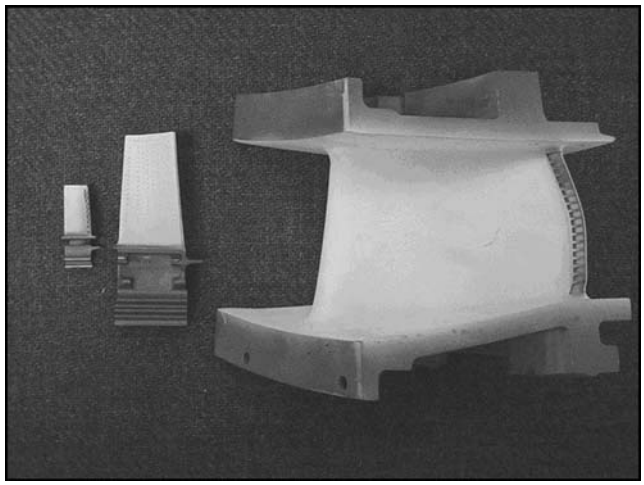

Fig. 19 Typical aircraft and IGT parts coated with EBPVD TBC. The part in the center is a CF6-80C2 1st stage HPT blade, the part on the left is a CF34 1st HPT blade, and the part on the right is a GE Power Systems Frame 6 Nozzle

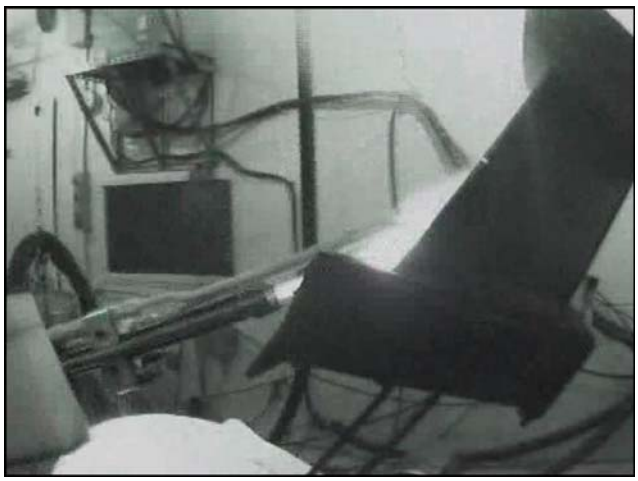

Fig. 18 A large IGT vane, with the trailing edge receiving an HVOF applied bond coating

Fig. 20 Platinum electroplating line, semi-automated

and by plating current and time. Uniformity of platinum thickness is critically important in controlling the microstructure of the coating. Typically 5-10 µm thick platinum is deposited in this process. The electroplated platinum is then diffused in a vacuum furnace prior to the aluminum diffusion.

Platinum plated parts are then loaded in a retort containing the aluminum donor and activator for VPA. Areas of parts not receiving coating, such as the roots of turbine blades, are masked by nickel paste or tape. Retorts are then placed in the hot zone of a furnace. A pre-determined time-temperature cycle is then followed. At the completion of this cycle, parts are demasked and cleaned before preparing for EBPVD TBC application. Figures 20 and 21 show a modern platinum electroplating line and a VPA furnace.

4.4.2 EBPVD TBC. EBPVD TBC coatings are produced by vacuum deposition of YSZ in a reactive atmosphere at elevated temperatures (approximately 1000 °C). Processing comprises the following steps:

The incoming parts are inspected and then typically cleaned in an ultrasonically enhanced aqueous or solvent cleaning process. Immediately before TBC coating, they receive a surface conditioning treatment, which also provides a clean oxide free metal surface.

TBC coating is done in an EBPVD vacuum coater. Parts are loaded into a vacuum chamber onto a manipulator. The chamber is then pumped down to vacuum and the parts manipulator transfers the load to a preheat chamber, where they are heated to approximately 1000 °C. During this preheating phase, the initial thin TGO forms to provide the necessary bond to the TBC.

The parts are then transferred to the coating chamber. 7YSZ ingot is evaporated by electron beams in vacuum and deposited onto the preheated parts. By a combination of rotation and tilting, a uniform coating over the airfoil surface is accomplished. Unwanted coating deposition is masked off by the fixturing. To compensate for some oxygen loss during coating, a minor amount of oxygen is added to the process. Typical deposition speeds are 2 to 6 μm per minute.

Fig. 21 VPA aluminizing furnace

After achieving the necessary coating thickness, the parts are retracted into the load chamber and cooled down. Normally, the as-coated surface finish is sufficient for engine use. Some critical parts receive an optional surface finish and optional age heat treatment. Final inspection checks for spits and pits from ingot eruptions and for chipped coating due to handling. Ancillary processes such as YSZ ingot conditioning, stripping of coating fixtures, and stripping of non-conforming hardware support the operation.

To cope with a wide product spectrum, it is critical that tooling can be changed within a short time to effectively coat part types with different coating thickness/coating time. This is accomplished by a 4-load chamber concept (Ref 37), as shown in Fig. 22.

A highly efficiency EBPVD production coater is shown in Fig. 23. The design allows having at any time one load of parts inside the coating chamber receiving a 7YSZ top layer.

5. Cost

The cost to coat an actual part with a modern TBC system is a complex function of many factors. These factors can be grouped into three cost categories:

A—One time cost factors

- Application development
- Tooling development and design
- Process qualification and approval
- Production process documentation

B—Direct coating related cost factors

- Direct materials (powder, ingot, plating salt, aluminizing donor ally)
- Auxiliary materials (grit, cleaning agent, gloves)
- Labor for

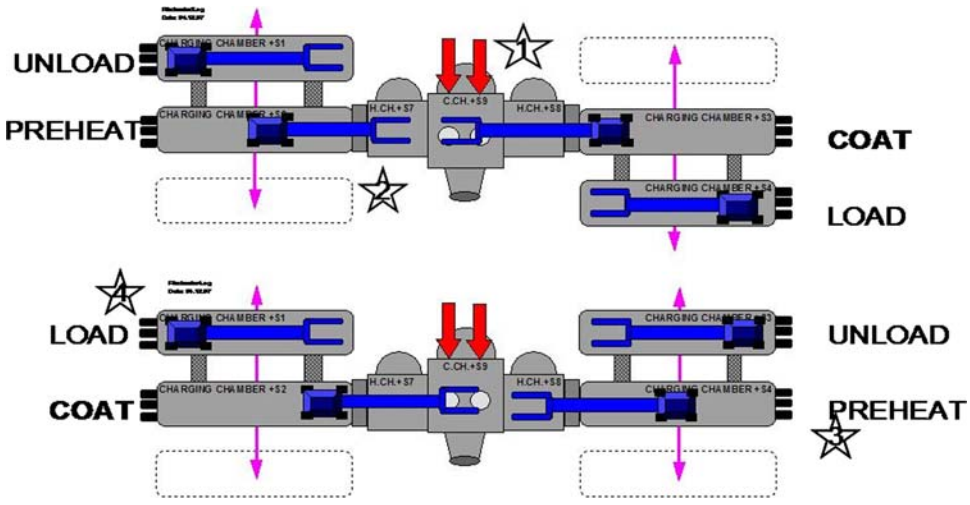

Fig. 22 Schematic operation with four load lock chambers (Courtesy of ALD Vacuum Technologies, Inc.)

Fig. 23 A 4-chamber EBPVD production coating system

Incoming inspection
Cleaning
Surface preparation (e.g., aqueous or solvent cleaning and grit blasting)
Fixturing and masking

- Post-coating processing (e.g., heat treatment)
- Equipment amortization
- Energy
- Process gases

C—Indirect cost factors (materials and services)

- Material preparation and recycling (e.g., ingot degassing)
- Preventive maintenance and spare parts
- Strip and rework in case of non-conformance
- Tooling cleaning and rework
- Tooling replacement
- Packing and shipping

Thus, the cost to coat an actual part is very much dependant on the part volume and the production life cycle of a part. The higher the volume and the longer the production life is, the less is the relative percentage of the one-time cost.

The actual coating process efficiency is also a tradeoff between process uniformity requirements and the process window. The wider the coating specification (within a reasonable range), the more economic is the coating process—especially in multipart batch operations such as EBPVD and diffusion aluminizing—since more parts can be coated at a time.

Tooling costs are also very process and part dependant. For thermal spray processing, stainless steel tooling material is usually sufficient, whereas for EBPVD and platinum aluminide diffusion, the higher operation temperatures require the use of superalloys. Tooling wear is essentially dependant on the tooling stripping process, with grit blasting in general more aggressive than wet stripping. A tooling fixture for an aero turbine blade typically costs several hundred dollars, whereas a fixture for an IGT bucket can cost three to five times as much.

With this variability in the cost elements, it can be misleading to state actual coating costs with precision. For each of the coating examples given above, it is more useful to state a typical range of costs related to various processing factors.

In a high-volume application, the one time costs become diluted, and the remaining key factors are:

- Equipment amortization
- Labor
- Direct materials (powder, ingot)
- Energy and process gas
- Indirect cost and material

5.1 Cost Structure for Selected Examples

In the following, these cost elements for selected examples are evaluated. Figure 24 exhibits the main cost groups B and C, as previously mentioned. For this cost breakdown, the following assumptions hold:

- An equipment amortization scheme of 10 years depreciation with a 10% annual interest rate.
- Material costs between \$30 and \$70 per kg for ceramic powder and ingot, and \$50 to 100 per kg for MCrAlY powder. The price for 1 oz Pt is above \$900.
- Energy costs are essentially site related, and are based on US averages.
- Gas prices of approximately \$0.1 to 0.2 per kg for CO_2, \$0.5 per m^3 for argon and \$1 to 2 per liter for kerosene.

5.2 Combustor Coating

The cost is determined by the size of the combustor and the surface area to be coated. Depending on the size of the combustor and the quantities, cost can range between several hundred and several thousand dollar per part. For the cost element breakdown, a mid-sized combustor and a coating thickness of 200 μm for the bond coat and 1 mm for the topcoat was used. For the investment, an APS plasma cell for approximately \$0.4 to 0.8 million was considered. Adding an automated parts handling system can add another \$0.5 to 0.8 million.

5.3 IGT Blade or Vane Coating

Necessary capital equipment includes a robotic spray booth, equipped with both HVOF and plasma torch/console systems, along with the necessary cleaning and grit blasting facilities. Also, masking and de-masking of the

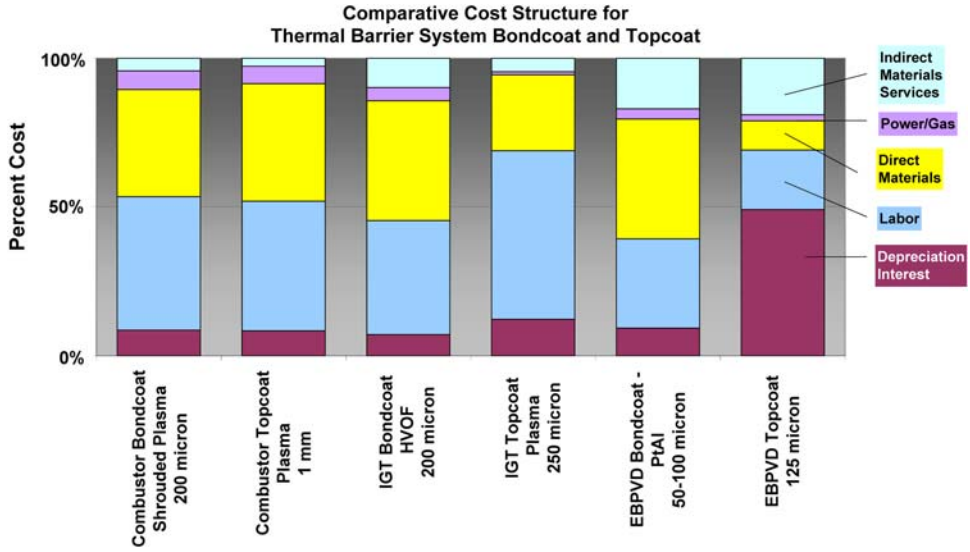

Fig. 24 Cost structure of selected coating applications. Direct materials are powder, platinum salt, and YSZ ingot. Labor assumes two persons per spray booth and ancillary services. Amortization assumes 10 years depreciation and 10% interest. Indirect materials and services include grit, cleaning agents, maintenance materials, etc.

cooling holes, which is a labor-intensive process, needs to be considered.

The high-deposition rates and relatively high-associated material costs, with the HVOF bond coat system, result in a cost breakdown where the material cost is the most significant portion of the cost. With APS TBC application, the relatively low-deposition rates and comparatively low-material expense, labor becomes the most significant portion of the cost. Thus, dependent on the blade or vane size, costs can range between several hundred and several thousand dollar per part. For the cost element breakdown, a coating thickness of 200 μm for the HVOF bond coat and 250 μm for the TBC topcoat was used.

5.4 EBPVD TBC on PtAl

A PtAl diffusion coating facility consisting of a platinum plating line, vacuum heat treat furnaces, and VPA diffusion furnaces costs between $3 million and $6 million. Equipment cost is the highest for EBPVD. Depending on the machine capacity, an EBPVD TBC facility costs between $15 million and $30 million.

For a given minimum platinum thickness requirement, the average thickness amount has to be increased in case of a part with a complex 3D shape and critical thickness locations. As a guideline, a typical aero blade 8 to 10 cm in length costs between $80 and $150 to aluminize. The same part is usually coated in batches of 12 per run in a large EBPVD coater. Depending on the coating thickness and the indirect coating factors previously discussed, a guideline for the coating cost is for EBPVD TBC only $120 to $200 per part. For larger aero parts with thicker coating requirements such as nozzle guide vanes, where only four to six parts can be coated in one batch, this cost easily triples. For the cost breakdown, a typical platinum aluminide thickness of 50 to 100 μm and an EBPVD TBC coating thickness of 125 μm is used.

6. Discussion

The cost of the thermal spray process, because of the relatively low equipment cost, is essentially driven by the material (powder) cost and labor cost. The material cost aspect is even more extreme in the case of platinum aluminide, where platinum can count for several $10 per part. In the case of EBPVD with the substantial equipment cost, the equipment depreciation calls for close to 50% of the overall production cost.

The relative contribution of these cost factors also provides guidance for application development for process and product optimization.

Processes with a high percentage of material cost demand improvement of the material utilization. In the case of thermal spray processes, optimized torch parameters can increase the material deposition efficiency substantially and need to be evaluated for each new application. In the case of platinum electroplating, the application development tends toward improving the uniformity and reproducibility of the platinum distribution. This allows adjusting the overall thickness in such a way that the specified thickness requirement is met even at critical locations without having to deposit an excessive thickness on uncritical locations.

Equipment amortization cost dictates the utilization of the facility. In the case of thermal spray processes, where the labor and material cost are the major cost factors, the equipment amortization is moderate; the equipment can be utilized in a one shift or two shift operations. In the case of expensive capital equipment

such as EBPVD and platinum aluminide, three shift operation is mandatory. In the case of EBPVD, development tends toward effective utilization of the expensive capital equipment.

7. Summary and Conclusion

The following state of the art processes for the deposition of TBC systems were compared:

- Shrouded plasma and HVOF for MCrAlY bond coat
- Plasma for low density YSZ and dense vertically cracked Zircoat
- Platinum aluminide diffusion coatings
- EBPVD TBC.

The key features of the coatings were outlined and compared.

The processing cost elements such as:

- Direct materials
- Labor
- Equipment amortization
- Energy and gas
- Indirect materials and services

have been evaluated and compared on an index basis for selected examples. The rough order of magnitude cost figures given for selected examples serve as a guideline; each application needs its own detailed evaluation considering all the elements as mentioned before.

In general, all presented technologies are considered to be mature. Still, substantial efforts are underway to improve quality and reduce cost by Lean Manufacturing and Six Sigma programs.

Acknowledgments

The authors would like to thank Dan Fillenwarth, Dan Helm, and Daming Wang for their input and valuable discussions.

References

1. S.M. Meier, D.K. Gupta, and K.D. Sheffler, Ceramic Thermal Barrier Coatings for Commercial Gas Turbine Engines, *J. Metal*, 1991, **43**(3), p 50-53
2. A. Maricocchi, A. Barz, and D. Wortman, PVD TBC Experience on GE Aircraft Engines, Thermal Barrier Coating Workshop, NASA Lewis Research Center, Cleveland, OH, March 27-29, NASA Conference Publication, 1995, 3312, p 79-90
3. D.V. Rigney, R. Viguie, D.J. Wortman, and D.W. Skelly, PVD Thermal Barrier Coating Applications and Process Development for Aircraft Engines, *J. Therm. Spray Technol.*, 1997, **6**(2), p 167
4. D. Zhu, J.A. Nesbitt, C.A. Barrett, T.R. McCue, and R.A. Miller, Furnace Cyclic Oxidation Behavior of Multicomponent Low Conductivity Thermal Barrier Coatings, *J. Therm. Spray Technol.*, 2004, **13**(1), p 84-92
5. D. Stöver, G. Pracht, H. Lehmann, M. Dietrich, J-E. Döring, and R. Vaßen, New Material Concepts for the Next Generation of Plasma-Sprayed Thermal Barrier Coatings, *J. Therm. Spray Technol.*, 2004, **13**(1), p 76-83
6. F.H. Stott, *Elevated Temperature Coatings, Science and Technology*, Vol. 11. The Minerals, Metals and Materials Society, 1996, p 151-161
7. *The Oxide Handbook*, G.V Samsonov, Ed., IFI/Plenum, New York, 1982
8. P.K. Wright and A.G. Evans, Mechanisms Governing the Performance of Thermal Barrier Coatings, *Curr. Opin. Solid State Mater. Sci.*, 1999, **4**, p 255-265
9. S. Alperine, M. Derrien, Y. Jaslier, and R. Mevrel, Thermal Barrier Coatings—The Thermal Conductivity Challenge, AGARD Report 823 "Thermal Barrier Coatings," 15-16 October 1997, p 1.1-1.10
10. V. Teixeira, M. Andritschky, H. Gruhn, W. Maliener, H.P. Buchkremer, and D. Stoever, Failure of Physically Vapor Deposition/Plasma-Sprayed Thermal Barrier Coatings During Thermal Cycling, *J. Therm. Spray Technol.*, 2000, **9**(2), p 191-197
11. J.A. Haynes, M.K. Ferber, and W.D. Porter, Thermal Cycling Behavior of Plasma-Sprayed Thermal Barrier Coatings with Various MCrAlX Bond Coats, *J. Therm. Spray Technol.*, 2000, **9**(1), p 38-48
12. E.H. Jordan, L. Xie, M. Gell, N.P. Padture, B. Cetegen, A. Ozturk, J. Roth, T.D. Xiao, and P.E.C. Bryant, Superior Thermal Barrier Coatings Using Solution Precursor Plasma Spray, *J. Therm. Spray Technol.*, 2004, **13**(1), p 57-65
13. T.A. Taylor, US Patent 5,073,433, Dec 17, 1991
14. T.A. Taylor, D.L. Appleby, A.E. Weatherill, and J. Griffiths, Plasma Sprayed Yttria-Stabilized Zirconia Coatings: Structure-Property Relationships, *Surf. Coat. Technol.*, 1990, **43/44**, p 470-480
15. A. Feuerstein and A. Bolcavage, Thermal Conductivity of Plasma and EBPVD Thermal Barrier Coatings, *Proceedings ASM International Surface Engineering Congress 2004*, Orlando, Florida
16. R.E. Taylor, Thermal Transport Property and Contact Conductance Measurements of Coatings and Thin Films, *Int. J. Thermophys.*, 1998, **19**(3), p 931-940
17. W. Chi, S Sampath, and H. Wang, Ambient and High-Temperature Thermal Conductivity of Thermal Sprayed Coatings, *J. Therm. Spray Technol.*, 2006, **15**(4), p 773-778
18. F. Cernuschi et al., Studies of the Sintering Kinetics of thick TBCs by Thermal Diffusivity Measurements, *J. Euro. Ceram. Soc.*, 2005, **25**, p 393-400
19. A. Flores Renteria et al., Effect of Morphology on Thermal Conductivity of EB-PVD PYSZ TBCs, *Surf. Coat. Technol.*, 2006, **201**, p 2611-2620
20. F.S Petit and G.W. Goward, Oxidation—Corrosion-Erosion Mechanisms of Environmental degradation of High Temperature Materials. *Coatings for High Temperature Processes*, E. Lang, Ed., Applied Science Publishers, 1985
21. R. Bouchet and R. Mevrel, Influence of Platinum and Palladium on Diffusion in bêta-NiAl phase, *Defect Diffusion Forum*, 2005, **237-240**, p 238-245
22. D.K Das, Vakil Singh, and S.V. Joshi, The Cylic Oxidation Performance of Aluminide and Pt-Aluminide Coatings on Cast i-Based Superalloy CM-247, *JOM-e*, **52**(1), 2000
23. F.P. Talboom et al., US Patent 3,542.530, Nov 24, 1970
24. D. Evans et al., US Patent 3,676,085, July 11, 1972
25. G.W. Goward et al., US Patent 3,754,903, Aug 28, 1973
26. Union Carbide Patent US 3,470,347, Sep 30, 1969
27. J. Foster et al., US patent 5,558,758, Sep 24, 1996 and 5,824,205, Oct 20, 1998
28. T. Koomparkping, S. Damrongrat, and P. Niranatlumpong, Al-Rich Precipitation in CoNiCrAlY Bondcoat at High Temperature, *J. Therm. Spray Technol.*, 2005, **14**(2), p 264-267
29. M. Schütze, *Corrosion and Environmental Degradation*, Vol. II, Wiley-VCH, 2000

30. A.W. Funkenbusch, J.G. Smeggil, and N.S. Bornstein, Reactive Element-Sulfur Interaction and Oxide Scale Adherence, *Metall. Trans.*, 1985, **16A**, p 1164-1166
31. J.G. Smeggil and A.J. Shuskus, The Oxidation Behavior of CoCrAlY, CoCrAl and Yttrium-Implanted CoCrAl Alloys Compared and Contrasted, *Surf. Coat. Technol.*, 1987, **32**, p 57-68
32. A.S. Kahn, C.E. Lowell, and C.A. Barrett, The Effect of Zirconium on the Isothermal Oxidation of Nominal Ni-14Cr-24Al Alloys, *J. Eelectrochem. Soc.*, 1980, **127**(3), p 670-679
33. J.R. Blachere, E. Schumann, G.H. Meier, and F.S. Pettit, Textures of Alumina Scales on FeCrAl Alloys, *Scripta Mater.*, 2003, **49**, p 909-912
34. N. Czech, F. Schmitz, and W. Stamm, Improvement of MCrAlY Coatings by Addition of Rhenium, *Surf. Coat. Technol. (Switzerland)*, 1994, **68/69**, p 17-21
35. J.L. Smialek, Improved Oxidation Life of Segmented Plasma Sprayed 8YSZ Thermal Barrier Coatings, *J. Therm. Spray Technol.*, 2004, **13**(1), p 66-75
36. M.H. Weatherly and R.C. Tucker, Union Carbide, US Patent 4,095,003, Jun 13, 1978
37. M. Mede, et al., New and Affordable Technical Solutions for Turbine Component Coatings, *Proceedings ASM International Surface Engineering Congress 2004*, Orlando, FL, p 189-196